On the role of entropy conservation and entropy loss governing substorm phases

J. Birn, M. Hesse, and K. Schindler

Abstract: MHD theory and simulations have shed light on the role of entropy conservation and loss during the course of a substorm. Entropy conservation appears to be a crucial element leading to the formation of thin embedded current sheets in the late substorm growth phase, causing the onset of an instability or a catastrophe (loss of equilibrium). Entropy loss (in the form of plasmoids) is essential in the earthward transport of flux tubes (bubbles, bursty bulk flows). Entropy loss may also change the tail stability properties and render ballooning modes unstable and thus contribute to cross-tail variability. We illustrate these effects through results from theory and simulations. We also verify that the entropy conservation as used in MHD remains a valid concept in particle simulations.

Key words: Entropy, Substorms.

1. Introduction

The large-scale dynamic evolution of the magnetosphere, including the substorm growth phase and the substorm expansion phase, is usually modeled by the one-fluid magnetohydrodynamic (MHD) equations. Major assumptions used in the derivation of the MHD equations from the more general framework of collisional or collisionless Vlasov/Boltzmann equations are (a) the neglect of the electric field in the plasma rest frame (ideal MHD),

$$\mathbf{E} + \mathbf{v} \times \mathbf{B} = 0 \tag{1}$$

(b) the assumption of isotropic plasma pressure p, and (c) the neglect of heat flux or, more narrowly, the divergence of the heat flux tensor. Here heat flux represents the third order moment of the particle distribution function, representing thermal energy transport in the plasma rest frame. This leads to the adiabatic, i.e., entropy conserving, law of state, which may be written as

$$\frac{d}{dt}\frac{p}{\rho^\gamma} = 0 \tag{2}$$

where $d/dt \equiv \partial/\partial t + \mathbf{v}\cdot\nabla$ is the time derivative in a comoving frame. Here $\gamma = 5/3$ is appropriate for an isotropic plasma distribution function (taken in the plasma rest frame), which also implies the absence of heat flux.

Although the details of substorm onset in the magnetotail are still a matter of debate, there is no doubt that magnetic reconnection, and plasmoid formation and ejection, play a crucial role in the expansive phase of substorms. This requires a local violation of the ideal MHD constraint (1) associated with a dissipative electric field

$$\mathbf{E}' = \mathbf{E} + \mathbf{v} \times \mathbf{B} \neq 0 \tag{3}$$

Received 18 June 2006.

J. Birn. Los Alamos National Laboratory, Los Alamos, New Mexico, USA
M. Hesse. NASA/Goddard Space Flight Center, Greenbelt, Maryland, USA
K. Schindler. Institut für Theoretische Physik, Ruhr-Universität Bochum, Bochum, Germany

In MHD simulations this is usually accomplished by some ad-hoc model of resistivity (or by numerical diffusion). In collisionless models appropriate for the magnetotail, resistivity from binary collisions does not play any role. Many of the investigations of magnetic reconnection in the magnetotail therefore have focused on the break-down of (1) and the properties of the dissipative electric field resulting particularly from electron inertia effects [14, 9, 11, 8, 13].

However, the entropy conservation (2) and its break-down also have important implications for the evolution of the magnetotail, the accessibility of certain states, and the stability of the tail. This is the topic of the present paper. In Sec. 2 we present results from quasi-static theory and MHD simulations that demonstrate the potential role of entropy conservation in the growth phase of substorms in governing thin current sheet formation and the loss of equilibrium. As discussed in Sec. 3, the subsequent loss of entropy by the severance of a plasmoid results in a ballooning unstable configuration. The entropy loss enables depleted flux tubes to penetrate close to the earth, while ballooning instability may provide cross-tail structure and filamentation. These results rely on the entropy conservation (2), which is imposed in the MHD model. However, as demonstrated in Sec. 4 from a comparison between an MHD simulation and a full particle simulation, the integral of entropy on moving flux tubes is well conserved in particle simulations as well, providing credence to the results of the MHD simulations.

2. Substorm growth phase: Thin current sheet formation, loss of equilibrium

In this section we discuss the possible role of entropy conservation during the substorm growth phase. Recently Birn and Schindler [3] investigated the quasi-static response of the magnetotail to a deformation of the magnetopause boundary, affecting particularly the inner tail. Using two-dimensional magnetohydrostatic (MHS) equilibium theory, together with flux, entropy, and topology conservation (equivalent to ideal MHD for slow, quasi-static, evolution), they demonstrated that a finite boundary deformation of magnetotail equilibria can lead to strong local current density enhancement, that is, the form-

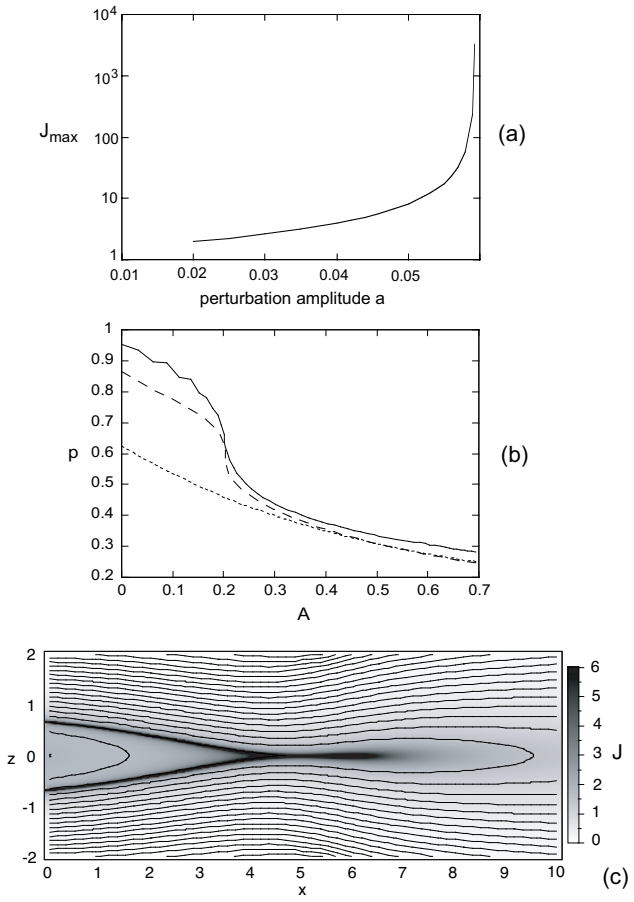

Fig. 1. (a) Maximum current density as function of the amplitude of the boundary indentation; (b) pressure as function of the flux variable A for the unperturbed state (dotted line), the theoretical limit obtained from quasi-static theory (dashed), and from an MHD simulation (solid line). Modified after [4]; (c) magnetic field configuration near the critical limit, consisting of a thin embedded current sheet (gray scale) that bifurcates toward the Earth (left).

ation of a thin current sheet. Equilibrium configurations that satisfy the constraints cease to exist when the boundary deformation exceeds a critical value.

Figure 1 illustrates this result. Panel (a) shows the maximum current density in the tail as a function of the amplitude of the boundary indentation a, which diverges at a finite value of a. Panel (b) shows the pressure P as a function of the magnetic flux variable A, where the magnetic field is given by $\mathbf{B} = \nabla A \times \hat{\mathbf{y}}$. The dotted line corresponds to the unperturbed state and the dashed line to the critical state, where $J = dP/dA$ becomes locally infinite. The solid line represents the result of an MHD simulation, where the critical state is obtained by a slow temporal evolution resulting from a temporal inflow through the boundary, which causes a similar deformation as in the quasi-static model [4]. Panel (c) illustrates the configuration near the critical state, showing an enlarged inner portion of the tail. A thin sheet with strongly enhanced current density (gray scale) becomes embedded in the plasma sheet. This sheet bifurcates into two sheets toward the Earth (to the left in Fig. 1).

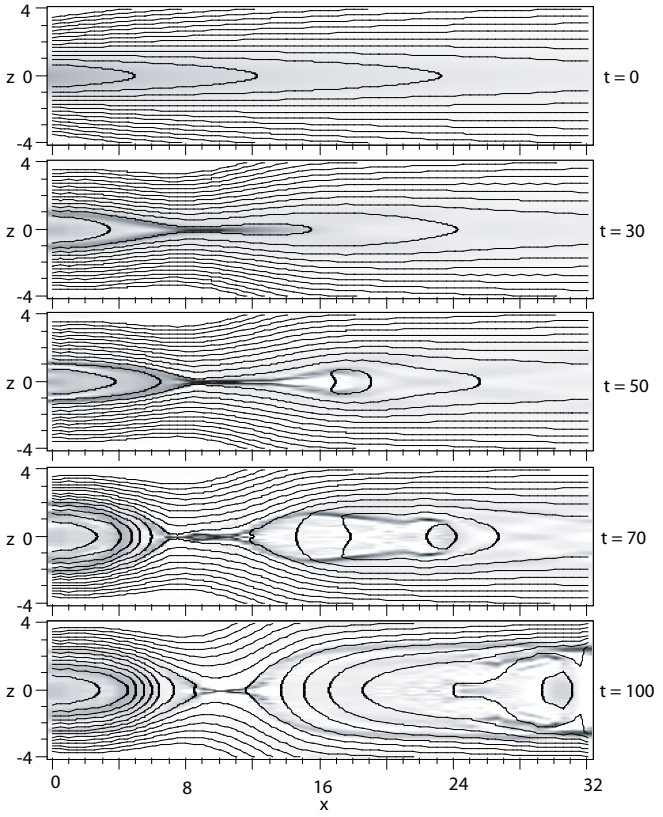

Fig. 2. MHD simulation of thin current sheet formation and plasmoid ejection in the tail, resulting from boundary deformation in the near tail. The gray scale indicates the current density.

3. Expansion phase: Role of reconnection, propagation of bubbles

The results of Sec. 2 showed the strong coupling between boundary perturbations, resulting from the impact of the solar wind, and current density intensification within a thin sheet forming within the plasma sheet. It is plausible that this leads to the onset of instability or the loss of equilibrium, regardless of the dissipation mechanism. In the presence of dissipation the strong current density enhancement is expected to cause reconnection. We simulated this by imposing finite, uniform, resistivity. As demonstrated by Fig. 2, this indeed leads to reconnection in the near tail and the formation and ejection of a plasmoid. Similar results can also be obtained from full particle simulations, where dissipation results from electron inertia causing nongyrotropy of the electron pressure tensor [7].

The plasmoid formation has a further consequence for closed field lines, connected with earth at both ends. Because parts of these field lines are severed, the remaining closed section becomes shorter and its total entropy content reduced. This is demonstrated in Fig. 3, showing the integrated quantity $S(A)$ defined by

$$S = \int p^{1/\gamma} dV = \int p^{1/\gamma} \frac{ds}{B} \tag{4}$$

where A is again the flux variable in the two-dimensional magnetic field, integrated at various times along field lines crossing the near-Earth boundary $x = 0$. A is normalized to 0 at

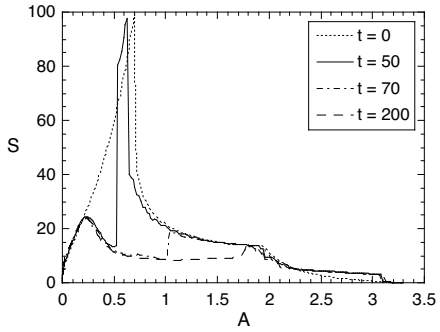

Fig. 3. Entropy function for the MHD simulation of Fig. 2 at various times indicated in the legend.

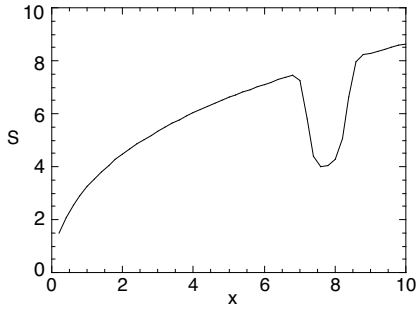

Fig. 4. Entropy function for a depleted flux tube (bubble).

$x = 0, z = 0$ and increases outward. The sharp decrease of the initial $S(A)$ (dotted line) near $A = 0.7$ marks the transition from closed to open field lines, which cross the far boundary $x = 32$, rather than the equatorial plane $z = 0$. In the absence of dissipation, that is, for vanishing resistivity, this function should be conserved. As a result of reconnection, however, $S(A)$ becomes reduced for field lines that are affected by reconnection. The sharp increase of $S(A)$ (near $A = 0.5$ for $t = 50$) marks the location of reconnection; it moves to higher A values, and from closed to open field lines, as time proceeds. Below this value the functions $S(A)$ show a deep minimum but remain essentially identical for the part that has undergone reconnection, that is, left of the steep jump. This shows that there is little further dissipation.

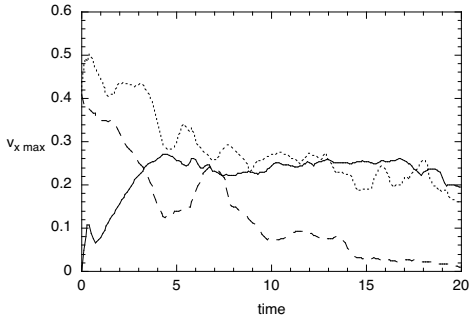

Fig. 5. Maximum earthward flow speed as function of time for bubbles with $y_m = 0.2$ and (a) pressure reduction but no initial velocity (solid line), (b) pressure reduction and initial velocity (dotted line), (c) no pressure reduction but finite initial velocity (dashed line). After [1].

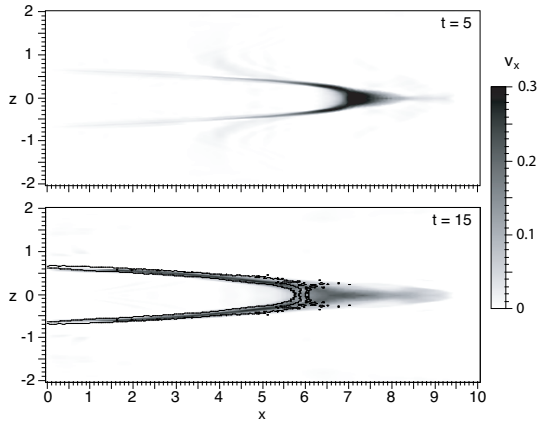

Fig. 6. Evolution of a entropy-depleted flux tube (bubble). The gray scale shows the earthward flow speed and the contours the boundary of the region of reduced entropy density in the x, z plane.)

As shown by [12], the nonmonotonic variation of the entropy function, resulting from the plasmoid loss, also changes the stability properties of the configuration and, specifically, the depleted flux tubes, which are often denoted a plasma "bubble" [10, 6]. The non-monotonic variation of the entropyleads to ballooning or interchange instability. Using three-dimensional magnetohydrodynamic simulations, Birn et al. [1] investigated the propagation of low-entropy bubbles in the magnetotail. To distinguish the role of the entropy depletion versus acceleration by reconnection, they studied the evolution of a closed magnetic flux tube with artificially reduced pressure (and thus entropy density). The initial entropy variation is shown in Fig. 4 and is qualitatively the same as in Fig. 3, resulting from reconnection. Birn et al. found that the depletion was crucial in permitting the earthward propagation of the bubble, reaching speeds of the order of 200-400 km/s, depending on the initial amount of depletion and the cross-tail extent of a bubble. Fig. 5 illustrates this result by a comparison of three simulations, one starting with a depleted flux tube (solid line), one with additional added initial earthward momentum (dotted line), and one with initial momentum but without depletion (dashed line). Obviously, simple acceleration without depletion does not lead to significant earthward propagation, whereas the two depleted flux tubes, after some initial phase, show similar evolution and propagation toward Earth. This result can be considered as the consequence of interchange instability, originally postulated by [10].

The instability of the depleted flux tube configuration against ballooning also leads to structuring of the depleted region in the cross-tail direction. This is demonstrated by Figs. 6 and 7, which show the earthward flow speed (gray scale) associated with the bubble at two different times in the x, z plane and the x, y plane, respectively. The top section shows the earthward propagation, confined within the depleted flux tube. The plots in the equatorial plane (bottom two panels), however, demonstrate that the bubble, which originally consists of a single connected flux tube, breaks apart into several pieces of flux tubes. This is the result of ballooning modes with a wave structure in the cross-tail direction.

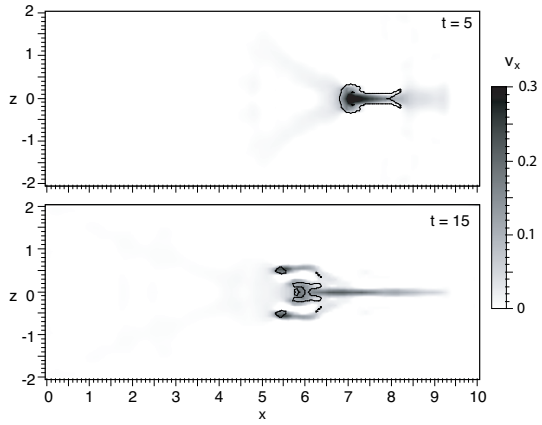

Fig. 7. Evolution of a entropy-depleted flux tube (bubble). The gray scale shows the earthward flow speed and the contours the boundary of the region of reduced entropy density in the x, y plane.)

4. Validity: Comparison between MHD and kinetic simulations

The results discussed in sections 2 and 3 are based on the entropy conservation (2), which is imposed in the MHD model. In a full kinetic model, this approximation may break down through the development of anisotropy and effects of heat conduction, in addition to reconnection. We have therefore investigated the conservation of entropy in a comparison of a particle simulation of magnetic reconnection with an MHD simulation [2]. This study was motivated by a recent comparative study of forced magnetic reconnection with various particle and fluid codes, named the "Newton challenge." In these simulations, the formation of a thin current sheet and magnetic reconnection are initiated in a plane Harris-type current sheet by temporally limited, spatially varying, inflow of magnetic flux (from top and bottom in Fig. 8). All simulations resulted in surprisingly similar final configurations [5] with a concentration of the current in rings around the center of the magnetic islands, as illustrated in Fig. 8. This suggested that entropy conservation operated similarly in fluid and particle codes despite the fact that kinetic approaches include anisotropy, a different dissipation mechanism, and different waves not included in MHD.

Specifically we investigated again the integral entropy measure $S(A)$, defined by Eq. (4), using a gauge in which A is frozen in the plasma outside the reconnection region. In the absence of dissipation and for vanishing heat flux (or, more generally, vanishing divergence of heat flux) $S(A)$ should be a conserved function. This function was evaluated for both a PIC simulation and an MHD simulation with localized resistivity given by

$$\eta = \eta_1 / \cosh^2 s \qquad s^2 = (x/d_x)^2 + (z/d_z)^2 \tag{5}$$

choosing $d_x = d_z = 1$ and $\eta_1 = 0.01$. Magnetic flux values A were derived from integrating $B_x = -\partial A/\partial z$ along the boundary $x = 16$. We note that, without dissipation, the flux values at the corners of the simulation box and, for symmetry reasons, at $x = \pm 16, z = 0$ should be conserved. We normalized A to vanish at $x = \pm 16, z = 0$, that is, at the o-type magnetic neutral points in the center of the evolving magnetic islands, where the plasma stays at rest.

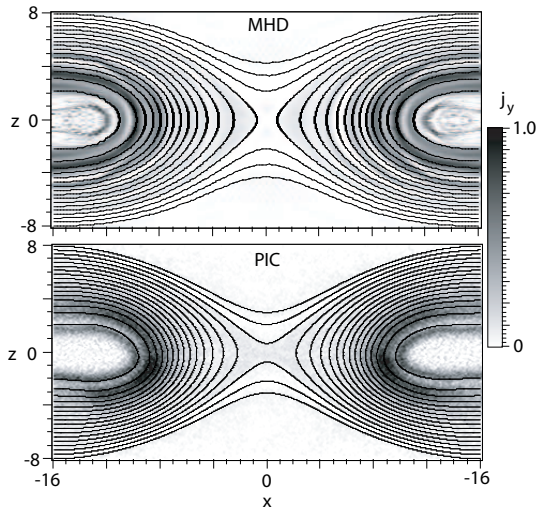

Fig. 8. Late magnetic field configuration and current density (gray scale) for an MHD (top) and a PIC simulation (bottom) of the Newton challenge problem [5, 2]. The outermost field lines are the ones that originally formed the boundaries $z = \pm 8$.To show the deformation more clearly, field lines outside of these are omitted.

With this gauge, the flux values should be frozen in the plasma fluid within the ideal MHD regime, that is, prior to and after reconnection. However, it makes sense also to compare the entropy before and after reconnection, because of the symmetry of the configuration and the fact that the entropy measure defined by (4) is an additive quantity. Thus we can compare the entropy measure S of a section of a field line that extends from the z axis to the boundary before reconnection with the corresponding field line that extends from the x axis to the boundary after reconnection.

Figure 9 (top) shows the entropy function (4) obtained in this way as function of the magnetic flux variable for both MHD and PIC simulations at the late stages of the simulations together with the initial distribution (dotted line). The bottom part of Figure 9 shows the corresponding pressure variations, also averaged over the field lines. For the PIC simulation the pressure p is defined by the trace of the full pressure tensor, given by

$$p = \frac{1}{3} p_{\parallel} + \frac{2}{3} p_{\perp} \tag{6}$$

For an indication of the anisotropy in the PIC simulation, the parallel and perpendicular components of the pressure tensor are shown as well as functions of A, again averaged over field lines.

The entropy functions in Figure 9 (top) show remarkable agreement with each other and with the initial distribution, despite the fact that most field lines at the late times have undergone reconnection. This demonstrates that the Joule dissipation at the reconnection site leads only to a minimal increase in the total entropy on a field line. In contrast, the pressure functions $P(A)$ have change drastically from the initial distribution but agree closely between MHD and PIC simulations. The small difference is largely due to the fact that the PIC simulation has evolved slightly more than the MHD simulation. The

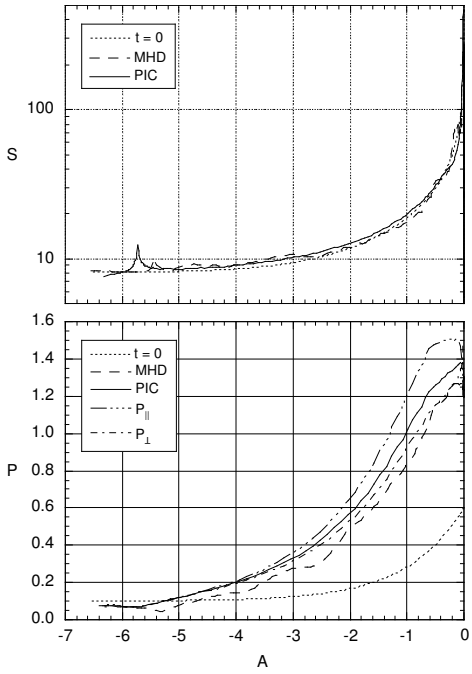

Fig. 9. Entropy (top) and pressure (bottom) as functions of the magnetic flux variable A for MHD (dashed line) and PIC simulations (solid line) of the Newton challenge problem [5]. Also shown are the parallel and perpendicular pressure components for the PIC simulation.

PIC simulation shows some anisotropy, particularly at values of A close to 0, which corresponds to the center of the magnetic islands.

The (approximate) entropy conservation through the reconnection process is a particular property that results from the symmetry of the Newton challenge problem with the x-point located at the center of the symmetrical box. This has the consequence that at the reconnection site a field line is split into two halves, which are then reconnected with symmetrical two halves, so that, in the absence of significant dissipation, the total entropy remains the same. In more general configurations without symmetry, such as the tail configuration of Fig. 2, only the sum of the entropies of the affected field lines would be conserved. That is, the entropy loss from a shortened reconnected field line corresponds to the entropy of the severed part contained within the plasmoid.

5. Summary and Discussion

We have discussed how entropy conservation and the loss of entropy might affect various substorm phases, including the growth phase, onset, and the expansion phase, in the magnetotail. Results from quasi-static theory and MHD simulations demonstrated how entropy conservation, together with flux and topology conservation in the growth phase of substorms governs thin current sheet formation and the loss of equilibrium. The strong current density intensification, which occurs when the critical state is approached, suggests the onset of instability or a catastrophe, that is, loss of equilibrium, regardless of the dissipation mechanism. This eventually leads to the onset of reconnection and plasmoid formation and ejection.

The subsequent loss of entropy by the severance of a plasmoid results in a ballooning or interchange unstable configuration. The loss of entropy is essential in enabling depleted closed flux tubes (bubbles) to penetrate to the inner magnetosphere closer to Earth, as suggested by [10]. Ballooning instability may also be responsible for providing cross-tail structure and filamentation of bubbles, which may be closely associated with localized fast flow bursts in the tail.

These results rely on the entropy conservation (2), which is imposed in the MHD model. However, as demonstrated by the comparison between an MHD simulation and a full particle simulation, the integral of entropy on moving flux tubes is well conserved in particle simulations as in MHD simulations, providing credence to the results of the MHD simulations. The (approximate) conservation of entropy, even through the reconnection process, is a consequence of the strong localization of Joule dissipation (given by $\mathbf{j} \cdot \mathbf{E}'$, where $\mathbf{E}' = \mathbf{E} + \mathbf{v} \times \mathbf{B}$) and of the lack of significant heat flux across the field.

Acknowledgments. This work was performed under the auspices of the US Department of Energy, supported by a grant from NASA Goddard Space Flight Center, and by NASA's Sun-Earth Connection Theory and Living With a Star Programs.

References

1. Birn, J., Hesse, M., and Schindler, K., On the propagation of bubbles in the geomagnetic tail, *Ann. Geophys.*, 22, 1773, 2004.
2. Birn, J., Hesse, M., and Schindler, K., Entropy conservation in simulations of magnetic reconnection, *Phys. Plasmas*, 2006, submitted.
3. Birn, J. and Schindler, K., Thin current sheets in the magnetotail and the loss of equilibrium, *J. Geophys. Res.*, 107, SMP18, doi:10.1029/2001JA0291, 2002.
4. Birn, J., Schindler, K., and Hesse, M., Formation of thin current sheets in the magnetotail: Effects of propagating boundary deformations, *J. Geophys. Res.*, 108, 1337, doi:10.1029/2002JA009641, 2003.
5. Birn, J., *et al.*, Forced magnetic reconnection, *Geophys. Res. Lett.*, 32, L06105, doi:10.1029/2004GL022058, 2005.
6. Chen, C. and Wolf, R., Interpretation of high-speed flows in the plasma sheet, *J. Geophys. Res.*, 98, 21409, 1993.
7. Hesse, M. and Schindler, K., The onset of magnetic reconnection in the magnetotail, *Earth Planets Space*, 53, 645, 2001.
8. Hesse, M. and Winske, D., Electron dissipation in collisionless magnetic reconnection, *J. Geophys. Res.*, 103, 26479, 1998.
9. Lyons, L. R. and Pridmore-Brown, D. C., Force balance near an X-line in a collisionless plasma, *J. Geophys. Res.*, 95, 20903, 1990.
10. Pontius, D. and Wolf, R. A., Transient flux tubes in the terrestrial magnetosphere, *Geophys. Res. Lett.*, 17, 49, 1990.
11. Pritchett, P. L., Effect of electron dynamics on collisionless reconnection in two-dimensional magnetotail equilibria, *J. Geophys. Res.*, 99, 5935, 1994.
12. Schindler, K. and Birn, MHD stability of magnetotail equilibria including a background pressure, *J. Geophys. Res.*, 109, A10208, doi10.1029/2004JA010537, 2004.

13. Shay, M. A. and Drake, J. F., The role of electron dissipation on the rate of collisionless magnetic reconnection, *Geophys. Res. Lett.*, 25, 3759, 1998.
14. Vasyli ̄unas, V. M., Theoretical models of magnetic fieldline merging, 1, *Rev. Geophys. Space Phys.*, 13, 303–336, 1975.